Bioorganic & Medicinal Chemistry Letters xxx (2016) xxx–xxx

Contents lists available at ScienceDirect

Bioorganic & Medicinal Chemistry Letters

journal homepage: www.elsevier.com/locate/bmcl

Synthesis of a selective HDAC6 inhibitor active in neuroblasts

Vincent Zwick [a], Claudia A. Simões-Pires [a], Alessandra Nurisso [a,b], Charlotte Petit [a], Carolina Dos Santos Passos [a], Giuseppe Marco Randazzo [a], Nadine Martinet [c], Philippe Bertrand [d,e], Muriel Cuendet [a,*]

[a] School of Pharmaceutical Sciences, University of Geneva, University of Lausanne, Rue Michel Servet 1, CH-1211 Geneva 4, Switzerland
[b] Département de Biochimie, Université de Montréal, H3C 3J7 Montréal, Québec, Canada
[c] Institut de chimie, UMR CNRS 7272, UNSA, F-06108 Nice, France
[d] Institut de Chimie des Milieux et Matériaux de Poitiers, UMR CNRS 7285, 4 rue Michel Brunet, TSA 521106, B28, 86073 Poitiers, France
[e] Réseau Epigénétique du Cancéropôle Grand Ouest, France

ARTICLE INFO

Article history:
Received 22 July 2016
Revised 1 September 2016
Accepted 4 September 2016
Available online xxxx

Keywords:
Histone deacetylases
Isoform selectivity
HDAC6
PAMPA
Neuroblastoma cells

ABSTRACT

In recent years, the role of HDAC6 in neurodegeneration has been partially elucidated, which led some authors to propose HDAC6 inhibitors as a therapeutic strategy to treat neurodegenerative diseases. In an effort to develop a selective HDAC6 inhibitor which can cross the blood brain barrier (BBB), a modified hydroxamate derivative (compound **3**) was designed and synthetized. This compound was predicted to have potential for BBB penetration based on in silico and in vitro evaluation of passive permeability. When tested for its HDAC inhibitory activity, the IC_{50} value of compound **3** towards HDAC6 was in the nM range in both enzymatic and cell-based assays. Compound **3** showed a cell-based selectivity profile close to that of tubastatin A in SH-SY5Y human neuroblastoma cells, and a good BBB permeability profile.

Abnormalities in protein acetylation levels caused by deregulation of HDAC/HAT activities are proposed to be involved in the pathogenesis of several diseases such as cancer, cardiovascular, and neurodegenerative disorders.[1–7] In light of this, HDACs have been considered to be pharmaceutical targets against these diseases. The search for HDAC inhibitors resulted in the identification and development of an increasing number of structurally diverse compounds able to inhibit HDAC isoforms with various potency and selectivity. This effort led to the FDA approval of the pan-HDAC inhibitors romidepsin, vorinostat, belinostat, and panobinostat as therapies for cancer treatment.[8,9]

The hypothesis that the acetylation status plays an important role in learning and memory processes, and seems to be impaired in neurodegeneration, led some authors to propose HDAC inhibitors as a therapeutic strategy to treat neurodegenerative diseases.[10] Among HDACs, HDAC6 presents several important roles in cell biology, especially its implication in the control of tubulin acetylation levels, which can make it a target for the discovery of drugs against neurodegeneration. The use of tubacin, a well-known HDAC6 inhibitor, increased the acetylation level of tubulin, which improved mitochondrial transport in hippocampal neurons.[11] This improvement restored learning and memory in a mouse model of Alzheimer's disease lacking HDAC6.[4] In this disease, HDAC6 inhibition also led to beneficial effects by acting on other protein targets such as tau, a protein which promotes assembly and stabilizes microtubules. In Alzheimer's disease, hyperphosphorylation of tau affects the regulation of axonal transport and results in the accumulation of neurofibrillary tangles causing neuronal dysfunction.[12] In 2014, Cook et al.[13] demonstrated that the use of ACY-738 (Fig. 1), a selective HDAC6 inhibitor able to cross the blood brain barrier (BBB), could decrease tau pathogenic hyperphosphorylation and aggregation by increasing its acetylation level in mice.

Therefore, the development of selective HDAC6 inhibitors is of great interest and the aim of the present study was to identify compounds able to selectively target HDAC6 in neuroblasts. Previously, the key role of the *tert*-butyloxycarbonyl (BOC) group in HDAC6 selectivity was demonstrated, suggesting the impact of this large lipophilic moiety on HDAC6 surface recognition. While compound **1** (Fig. 1) did not show a significant selectivity for HDAC6, its BOC derivative **2** selectively inhibited this isoform.[14] Considering these data and the growing interest in identifying HDAC6 selective inhibitors, compounds **1** and **2** were first studied by using an in silico approach to assess their potential ability to cross the BBB and to match optimal CNS physicochemical features according to the

* Corresponding author. Tel.: +41 22 379 3386; fax: +41 22 379 3399.
E-mail address: muriel.cuendet@unige.ch (M. Cuendet).

http://dx.doi.org/10.1016/j.bmcl.2016.09.011
0960-894X/

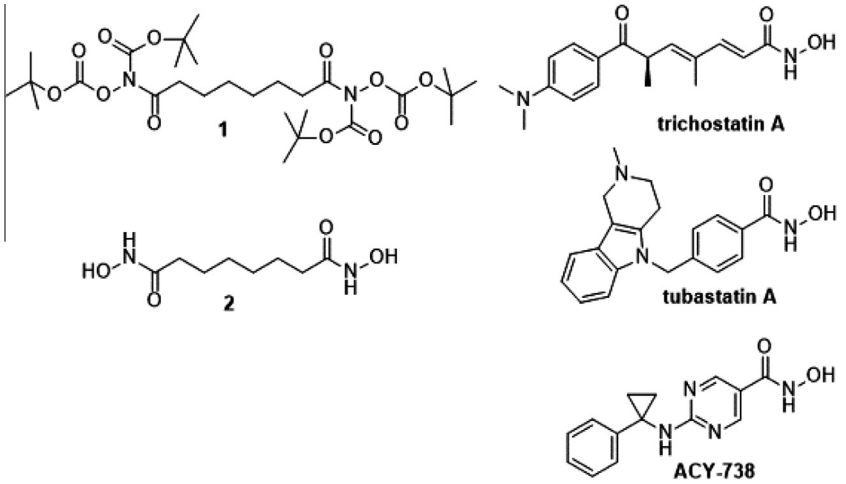

Figure 1. Chemical structures of compounds **1** and **2**, and other compounds used in this work for comparison purposes.

rules described by Pajouhesh et al.,[15] and by Wager et al. (Table S1).[16]

By combining information coming from those studies, it is clear that BBB penetration is strongly influenced by six fundamental physicochemical properties: *C*log*P*, *C*log*D*, molecular weight (MW), topological polar surface area (TPSA), number of hydrogen bond donors (HBD), and pK_a. For each of them, a desirable range is reported. Whereas compounds **1** and **2** did not satisfy the described criteria for BBB crossing, compound **3** was the most promising one (Table S1). Indeed, pK_a values reflect the difficulty of strong acids and bases to penetrate the BBB. Compound **3** is characterized by a hydroxamate chelating group with a predicted pK_a of 8.9. Pajouhesh et al.[15] proposed to limit pK_a for BBB penetration between 4 and 10, whereas pK_a values equal or lower than 8 were the limits proposed by Wager et al.[16] Hydroxamates have already been reported in the literature to be active on CNS. For example, tubastatin A (predicted pK_a of 9.8), is one of the most promising HDAC6 selective inhibitors developed so far with strong neuroprotective properties (Fig. 1).[17–20]

The use of cross metathesis has been previously validated to synthesize compounds **1** and **2**,[21] and was applied to synthetize derivative **3** (Scheme 1), aiming at achieving both HDAC6 selectivity and optimal CNS targeting features. In compound **3**, one of the two hydroxamate moieties was kept for assuring zinc chelation, while the other one was replaced by a bulky 1,3-benzodioxole as a cap group to address HDAC6 selectivity. Finally, the linker was shortened to mimic tubastatin A features. Cross metathesis was used to synthesize compound **3** from safrol (**4**) and the known intermediate **5** (Scheme 1).[21] A multistep synthesis of benzo[1,3]-dioxole with polyunsaturated alkene chain was described to give micromolar HDAC inhibitors (Scheme 1),[22] but saturated ones are unknown. Optimized condition for cross metathesis with Grubbs 1st generation catalyst was thus used to produce new HDAC inhibitors bearing this benzo[1,3]dioxole from safrol (**4**). The method consisted in preparing two CH_2Cl_2, solutions: one containing the two alkenes **4** and **5**, and the other the Grubbs 1st generation catalyst. The catalyst solution was added slowly at 0.5 ml/h in an already refluxing solution of alkenes. Once the catalyst addition was over, reflux was maintained for one more hour. The ratio of compounds **4**:**5** was first set to 1:2. In the previously optimized conditions for symmetric metathesis, the two possible symmetric cross products **6** and **7** and the desired dissymmetric one **8** were

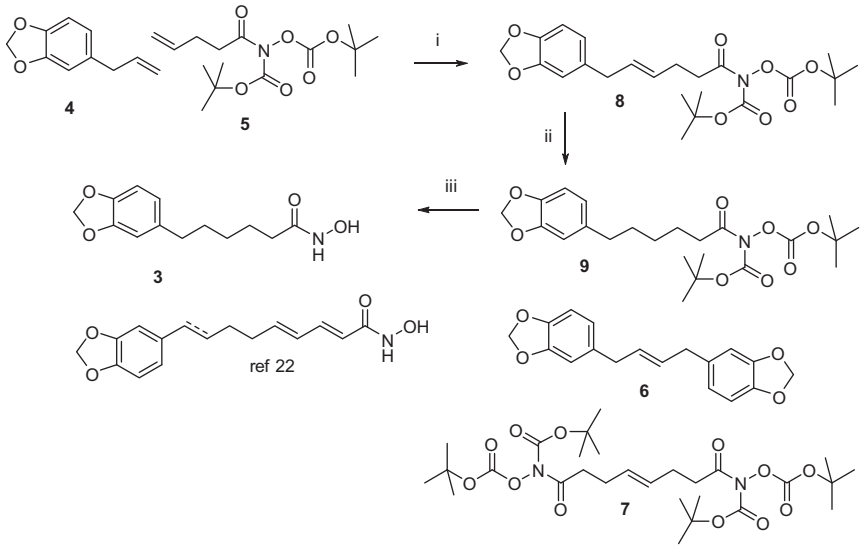

Scheme 1. Regents and conditions: (i) 7.5% mol. Grubbs 1st generation catalyst, refluxing CH_2Cl_2, 7 h, 59% (ii) H_2, Pd/C 10%, EtOAc, room temperature, 66%, (iii) TFA, CH_2Cl_2, room temperature, 95%.

Please cite this article in press as: Zwick, V.; et al. *Bioorg. Med. Chem. Lett.* (2016), http://dx.doi.org/10.1016/j.bmcl.2016.09.011

obtained in a 1:3.7:3.5 ratio. Due to significant differences in polarity, compounds could be easily separated by conventional flash chromatography. The desired compound **8** was isolated with 59% yield. Modifying the ratio of the starting compounds **4**:**5** to 2:1 gave an analogous products ratio, with a slight decrease in the desired compound **8** (59–55%). These results illustrated the higher reactivity of **4** that was unaffected by the ratio of starting material compared to **5**. Using a 1:1 ratio for **4**:**5** seemed to be less interesting as it resulted in a yield of only 33% for **8**. As previously described, reduction of **8** gave intermediate **9** (66% isolated yield), and TFA deprotection afforded the desired compound **3** (95% isolated yield).

Compound **3** was tested for its HDAC inhibitory activity, by using either HeLa nuclear extracts containing a mixture of nuclear HDAC isoforms (mainly HDAC1, HDAC2, and HDAC3), or HDAC1 and HDAC6 recombinant enzymes. This compound showed a similar potency towards HDAC6 than that observed for tubastatin A; however, its HDAC6 selectivity over HDAC1 was lower (Table 1). Furthermore, the selectivity index of compound **3** was around 15 for HDAC6 versus HDAC1 inhibition, while tubastatin A showed a much higher selectivity (>57), when tested on purified enzymes, as already reported in the literature.[17] Despite this, the high activity of compounds **3** against HDAC6 raised the question on how permeable, potent and selective compound **3** would be in living cells in comparison to tubastatin A.

Compound **3** and tubastatin A fulfilled the physicochemical requirements proposed by Pajouhesh et al.[15] and by Wager et al.,[16] suggesting that it may cross the BBB and reach the CNS (Table S1). This prediction was further corroborated in vitro by a Parallel Artificial Membrane Permeability Assay (PAMPA). This is a well-established assay used to predict the transcellular passive absorption through biological barriers.[23] In this study, the reference method PAMPA-BBB[24] was chosen to evaluate the passive BBB permeation of compound **3** in comparison to **1** and **2**. The percentage of compound that was retained by the artificial membrane (membrane retention, MR) and the speed at which the compound had crossed it (effective passive permeability value P_e in cm/s) were calculated. The P_e value of compound **3** was 8.7×10^{-6} cm/s (Table 2). As reported in the original method,[24] a P_e value of 4.0×10^{-6} cm/s corresponds to CNS+ compounds. This result showed the potential of compound **3** to reach the brain via the transcellular passive route, which is the most straightforward and non saturable mechanism for BBB penetration. Moreover, the passive permeability of compound **3** was higher than tubastatin A, suggesting that **3** is a better candidate to selectively inhibit HDAC6 in models of neurodegeneration. Compounds **1** and **2** were not permeable in the PAMPA-BBB method (Table 2), corroborating the in silico predicted lack of permeability. The PAMPA-BBB was also recently reported to predict the phospholipidosis risk, which is characterized by the gradual accumulation of drug-phospholipid complexes in tissues, a known cause of cell toxicity.[25,26] The MR represents the affinity of a tested drug for the lipidic artificial membrane compared to the buffer and is therefore used to characterize the formation of drug/phospholipid complexes. The MR of compound **3** was lower than 30% (Table 2), suggesting a weaker potency to induce phospholipidosis[26] in comparison to tubastatin A (Table 2). These results are important insights on the bioavailability and safety of compound **3**.

Table 2
PAMPA effective permeability (P_e) and membrane retention (MR) values of compounds **1**–**3** and tubastatin A

Compound	$P_e \times 10^{-6}$ (cm/s)	MR (%)
1	<2	<1
2	<2	<1
3	8.7 ± 0.6	6.8 ± 0.6
Tubastatin A	6.8 ± 2.7	70.8 ± 11.3

To investigate whether the selectivity profile of the new derivative was maintained in cells, compound **3** was tested on SH-SY5Y human neuroblastoma cells, which have been widely used to develop neuronal models of neurodegeneration.[27–30] The cell-based assay used in the present study consisted in incubating cells for 8 h with test samples or vehicle, together with a general HDAC substrate (MAL), an HDAC1-selective substrate (MOCPAC), or an HDAC6-selective substrate (BATCP). The substrates and their deacetylated products were then analyzed by a UHPLC system coupled to ESI-MS/MS in MRM mode. This approach offers the possibility to monitor the activity of both HDAC1 and HDAC6 in cells. It takes into account the specific behavior and expression level of each HDAC isoform, and gives a selectivity profile correlating with results obtained when using endogenous HDAC substrates.[14] In this assay, tubastatin A was less selective towards HDAC6 in SH-SY5Y cells (Table 3) than when tested against isolated enzymes (Table 1). This phenomenon is not unique: HDAC inhibitors can display various selectivity profiles between enzymatic and cell-based assays. It is the case for compound ST-3595, which showed an enzymatic selectivity towards HDAC6 that was not observed in cells.[31] More interestingly, compound **3** displayed a cell-based selectivity index towards HDAC6 close to the one of tubastatin A (Table 3).

Subsequently, docking studies were carried out on HDAC1 PDB id 4BKX[32] and HDAC6 (homology model) catalytic sites to understand the binding mode of compound **3** into these two isoforms, and to explain its selectivity towards HDAC6. The molecular docking protocol was first validated through the re-docking of vorinostat (SAHA) within the HDAC1 and HDAC6 protein structures. GOLD docking algorithm coupled with ASP score (CCDC, Cambridge, UK) was able to retrieve a meaningful position of SAHA into the catalytic site of each isoform (Fig. S1).[17] Compound **3** was then docked into HDAC1 and HDAC6 catalytic sites using the validated docking methodology. The hydroxamate group of compound **3** chelated the

Table 1
IC_{50} values of compound **3**, tubastatin A and trichostatin A (TSA) for HDAC inhibition using HeLa nuclear extract, HDAC1 and HDAC6

Compound	IC_{50}[a] (nM)			Selectivity index[e]
	HeLa nuclear extract[b]	HDAC1[c]	HDAC6[d]	
3	188.1 ± 19.9	560.1 ± 29.3	36.7 ± 0.99	15.3
Tubastatin A	>2000	>2000	34.9 ± 1.4	>57.3
TSA[f]	5.9 ± 0.42	15.7 ± 1.5	16.0 ± 0.74	0.98

[a] Values are shown as mean ± SD of three independent experiments in triplicate.
[b] Calculated by measuring the MAL substrate and its deacetylated product.
[c] Calculated by measuring the MOCPAC substrate and its deacetylated product.
[d] Calculated by measuring the BATCP substrate and its deacetylated product.
[e] Selectivity index defined as the ratio IC_{50} HDAC1/IC_{50} HDAC6.
[f] Positive control.

Please cite this article in press as: Zwick, V.; et al. *Bioorg. Med. Chem. Lett.* (2016), http://dx.doi.org/10.1016/j.bmcl.2016.09.011

Table 3
IC_{50} values of compound **3**, TSA and tubastatin A in SH-SY5Y human neuroblastoma cells using substrates for general HDAC, HDAC1, and HDAC6

Compound	IC_{50}[a] (nM)			Selectivity index[e]
	General HDAC[b]	HDAC1[c]	HDAC6[d]	
3	310.4 ± 11.8	973.1 ± 5.9	164.2 ± 3.3	5.9
Tubastatin A	122.1 ± 3.6	1109.7 ± 72.1	94.3 ± 3.2	11.8
TSA	9.1 ± 0.33	18.8 ± 0.91	7.8 ± 0.76	2.4

[a] Values are shown as mean ± SD of three independent experiments in triplicate.
[b] Calculated by measuring the MAL substrate and its deacetylated product.
[c] Calculated by measuring the MOCPAC substrate and its deacetylated product.
[d] Calculated by measuring the BATCP substrate and its deacetylated product.
[e] Selectivity index defined as the ratio IC_{50} HDAC1/IC_{50} HDAC6.

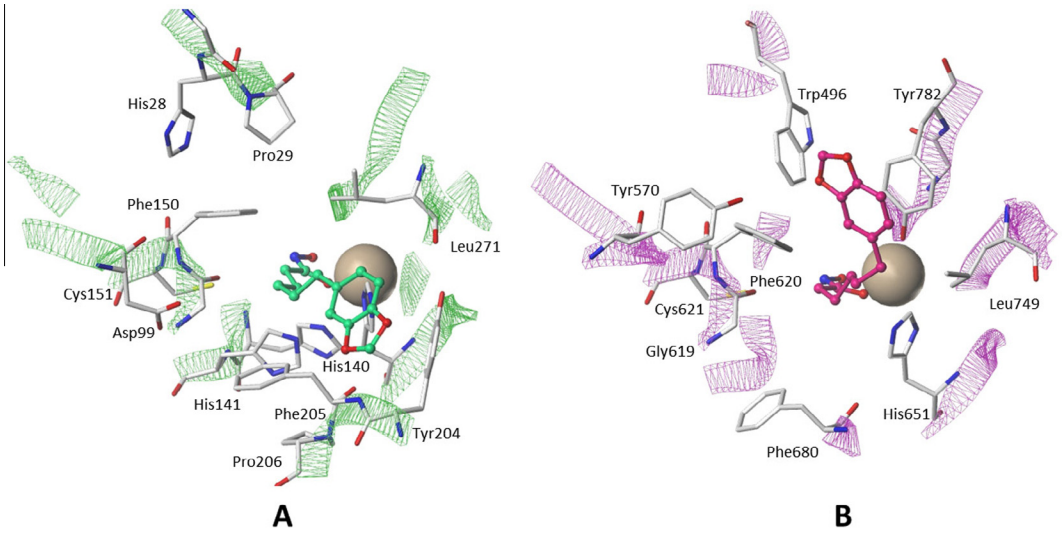

Figure 2. Molecular docking results. Best-ranked docking poses of compound **3** (balls & sticks atoms) in complex with HDAC1 (green ribbons, ASP score 45.0, A) and HDAC6 (magenta ribbons, ASP score 43.4, B). Residues characterizing the binding site are represented as sticks and labeled in black.

zinc ion of both isoforms, and the linker, shorter than the one of SAHA but mimicking the one of tubastatin A,[17] was stabilized by van der Waals interactions through hydrophobic residues characterizing the HDAC tunnel. Hydrophobic contacts between the benzodioxole moiety of compound **3** and HDAC1 Phe205, Tyr204, and Leu271 side chains were detected. The benzodioxole group was found to be trapped in a hydrophobic and electronically rich niche of HDAC6, composed of bulky residues (Phe620, Tyr782, and Trp496). According to the experimental data (Tables 1 and 3), compound **3** showed some degree of selectivity towards HDAC6. This may be due to the presence of the benzodioxole group able to target the hydrophobic HDAC6 channel rim (Fig. S2).[17] This moiety was found to be stabilized by a π–π sandwich between HDAC6 Phe620 and Tyr782 side chains, not present in HDAC1 (Fig. 2). This result was also confirmed by further molecular docking calculations conducted on the very recent crystallographic structure of the catalytic domain of HDAC6 (Fig. S3).[33]

In conclusion, an HDAC inhibitor (compound **3**) with ~10-fold HDAC6 selectivity over HDAC1 was designed and synthesized. This compound was predicted to have potential for BBB penetration based on in silico and in vitro evaluation of BBB passive permeability, comparable to currently available hydroxamates. Compound **3** showed HDAC6 selectivity over HDAC1 in both enzymatic and cell-based assays using SH-SY5Y human neuroblastoma cells, in which its selectivity profile was close to that of tubastatin A. Docking studies of compound **3** in HDAC1 and HDAC6 catalytic sites suggested that the benzodioxole group played an important role for the HDAC6 inhibitory activity by interacting with its hydrophobic channel rim. This selectivity profile and the involvement of HDAC6 within the pathogenesis mechanism of several neuronal disorders such as Alzheimer, Parkinson and Huntington diseases makes this compounds a good candidate to be tested in neurodegeneration models.

Acknowledgments

Authors thank the Centre National de la Recherche Scientifique, University of Poitiers, Region Poitou-Charentes (FEB grant), the Ligue Contre le Cancer: committees of Vendée, et Charente-Maritime, and COST Actions CM1106 and CM1406 for financial support. AN thanks the Excellence programme of the University of Geneva and the Swiss National Science Foundation (P300P3_158507) for financial support.

Supplementary data

Supplementary data (material and methods for the syntheses and characterization of compounds, HDAC inhibition assays, PAMPA-BBB assay and molecular modeling) associated with this article can be found, in the online version, at http://dx.doi.org/10.1016/j.bmcl.2016.09.011.

References and notes

1. Stubbs, M. C.; Kim, W.; Bariteau, M.; Davis, T.; Vempati, S.; Minehart, J.; Witkin, M.; Qi, J.; Krivtsov, A. V.; Bradner, J. E.; Kung, A. L.; Armstrong, S. A. *Clin. Cancer Res.* **2015**, *21*, 2348.
2. Colarossi, L.; Memeo, L.; Colarossi, C.; Aiello, E.; Iuppa, A.; Espina, V.; Liotta, L.; Mueller, C. *Proteom. Clin. Appl.* **2014**, *8*, 924.

3. Kang, Z. H.; Wang, C. Y.; Zhang, W. L.; Zhang, J. T.; Yuan, C. H.; Zhao, P. W.; Lin, Y. Y.; Hong, S.; Li, C. Y.; Wang, L. *PLoS ONE* **2014**, *9*, e98894.
4. Govindarajan, N.; Rao, P.; Burkhardt, S.; Sananbenesi, F.; Schlüter, O. M.; Bradke, F.; Lu, J.; Fischer, A. *EMBO Mol. Med.* **2013**, *5*, 52.
5. Kilgore, M.; Miller, C. A.; Fass, D. M.; Hennig, K. M.; Haggarty, S. J.; Sweatt, J. D.; Rumbaugh, G. *Neuropsychopharmacology* **2010**, *35*, 870.
6. Simões-Pires, C.; Zwick, V.; Nurisso, A.; Schenker, E.; Carrupt, P.-A.; Cuendet, M. *Mol. Neurodegener.* **2013**, *8*, 1.
7. Donmez, G.; Outeiro, T. F. *EMBO Mol. Med.* **2013**, *5*, 344.
8. West, A. C.; Johnstone, R. W. *J. Clin. Invest.* **2014**, *124*, 30.
9. Lee, H. Z.; Kwitkowski, V. E.; Del Valle, P. L.; Ricci, M. S.; Saber, H.; Habtemariam, B. A.; Bullock, J.; Bloomquist, E.; Shen, Y. L.; Chen, X. H.; Brown, J.; Mehrotra, N.; Dorff, S.; Charlab, R.; Kane, R. C.; Kaminskas, E.; Justice, R.; Farrell, A. T.; Pazdur, R. *Clin. Cancer Res.* **2015**, *21*, 2666.
10. Falkenberg, K. J.; Johnstone, R. W. *Nat. Rev. Drug. Disc.* **2014**, *13*, 673.
11. Chen, S.; Owens, G. C.; Makarenkova, H.; Edelman, D. B. *PLoS ONE* **2010**, *5*, e10848.
12. Iqbal, K.; Liu, F.; Gong, C. X.; Grundke-Iqbal, I. *Curr. Alzheimer Res.* **2010**, *7*, 656.
13. Cook, C.; Carlomagno, Y.; Gendron, T. F.; Dunmore, J.; Scheffel, K.; Stetler, C.; Davis, M.; Dickson, D.; Jarpe, M.; DeTure, M.; Petrucelli, L. *Hum. Mol. Genet.* **2014**, *23*, 104.
14. Zwick, V.; Simões-Pires, C.; Cuendet, M. *J. Enzyme Inhib. Med. Chem.* **2016**, *5*, 1.
15. Pajouhesh, H.; Lenz, G. R. *NeuroRx* **2005**, *2*, 541.
16. Wager, T. T.; Hou, X.; Verhoest, P. R.; Villalobos, A. *ACS Chem. Neurosci.* **2010**, *1*, 435.
17. Butler, K. V.; Kalin, J.; Brochier, C.; Vistoli, G.; Langley, B.; Kozikowski, A. P. *J. Am. Chem. Soc.* **2010**, *132*, 10842.
18. Zhang, L.; Liu, C.; Wu, J.; Tao, J. J.; Sui, X. l.; Yao, Z. G.; Xu, Y. F.; Huang, L.; Zhu, H.; Sheng, S. L. *J. Alzheimers Dis.* **2014**, *41*, 1193.
19. d'Ydewalle, C.; Krishnan, J.; Chiheb, D. M.; Van Damme, P.; Irobi, J.; Kozikowski, A. P.; Berghe, P. V.; Timmerman, V.; Robberecht, W.; Van Den Bosch, L. *Nat. Med.* **2011**, *17*, 968.
20. Selenica, M. L.; Benner, L.; Housley, S. B.; Manchec, B.; Lee, D. C.; Nash, K. R.; Kalin, J.; Bergman, J. A.; Kozikowski, A.; Gordon, M. N.; Morgan, D. *Alzheimers Res. Ther.* **2014**, *6*, 1.
21. Zwick, V.; Nurisso, A.; Simões-Pires, C.; Bouchet, S.; Martinet, N.; Lehotzky, A.; Ovadi, J.; Cuendet, M.; Blanquart, C.; Bertrand, P. *Bioorg. Med. Chem. Lett.* **2016**, *26*, 154.
22. Luo, Y.; Liu, H. M.; Su, M. B.; Sheng, L.; Zhou, Y. B.; Li, J.; Lu, W. *Bioorg. Med. Chem. Lett.* **2011**, *21*, 4844.
23. Avdeef, A. In *Absorption and Drug Development*; John Wiley & Sons: Hoboken, NJ, USA, 2003; pp 116–246.
24. Di, L.; Kerns, E. H.; Fan, K.; McConnell, O. J.; Carter, G. T. *Eur. J. Med. Chem.* **2003**, *38*, 223.
25. Balogh, G. T.; Müller, J.; Könczöl, Á. *Eur. J. Pharm. Sci.* **2013**, *49*, 81.
26. Ceccarelli, M.; Germani, R.; Massari, S.; Petit, C.; Nurisso, A.; Wolfender, J.-L.; Goracci, L. *Colloids Surf., B. Biointerfaces* **2015**, *136*, 175.
27. Xie, H. R.; Hu, L. S.; Li, G. Y. *Chin. Med. J.* **2010**, *123*, 1086.
28. Lopes, F. M.; Schröder, R.; da Frota Júnior, M. L. C.; Zanotto-Filho, A.; Müller, C. B.; Pires, A. S.; Meurer, R. T.; Colpo, G. D.; Gelain, D. P.; Kapczinski, F.; Moreira, J. C. F.; da Cruz Fernandes, M.; Klamt, F. *Brain Res.* **2010**, *1337*, 85.
29. Borland, M. K.; Trimmer, P. A.; Rubinstein, J. D.; Keeney, P. M.; Mohanakumar, K.; Liu, L.; Bennett, J. P., Jr. *Mol. Neurodegener.* **2008**, *3*, 1326.
30. Gómez-Santos, C.; Ferrer, I.; Santidrián, A. F.; Barrachina, M.; Gil, J.; Ambrosio, S. *J. Neurosci. Res.* **2003**, *73*, 341.
31. Milli, A.; Perego, P.; Beretta, G. L.; Corvo, A.; Righetti, P. G.; Carenini, N.; Corna, E.; Zuco, V.; Zunino, F.; Cecconi, D. *J. Proteome Res.* **2011**, *10*, 1191.
32. Millard, C. J.; Watson, P. J.; Celardo, I.; Gordiyenko, Y.; Cowley, S. M.; Robinson, C. V.; Fairall, L.; Schwabe, J. W. *Mol. Cell* **2013**, *51*, 57.
33. Hai, Y.; Christianson, D. *FASEB J.* **2016**, *30*, 1083.